An integrated solution for rapid biosensing combining linker free binding, freeze drying and high sensitivity ellipsometric detection

Yongbai Yin[1], David.R. McKenzie[1], Keith Fisher[2], Chuan Guo[3], Neil Nosworthy[1], Marcela .M.M. Bilek[1]

[1]School of Physics, University of Sydney, NSW 2006, Australia
[2]School of Chemistry, University of Sydney, NSW 2006, Australia
[3]School of Biochemical Engineering, University of Sydney, NSW 2006, Australia

Abstract

A novel integrated biosensor methodology is proposed and demonstrated. The methodology utilizes a nitrogen-containing plasma polymer to achieve linker-free binding of biorecognition molecules that allows the sensor surface to be freeze dried for long shelf life under ambient conditions. The sensor is configured for single wavelength ellipsometric detection providing a low cost, versatile, and rapid sensing and diagnosis platform suitable for a wide range of applications and end-users. The merits of the methodology were demonstrated using three antigen-antibody pairs.

Introduction

Biosensing using a biological recognition element is the preferred approach to identify and quantify biologically-relevant analytes. Suitable approaches that have been demonstrated using biological recognition elements include antigen-antibody interactions[1,2], oligonucleotides[3,4], lectin-glycoprotein and hormone-receptor interactions[5, 6]. In these interactions, molecular binding or detaching is quantified or sensed using a transducer. Proposed sensing techniques include scattering interferometry[7], microcantilevers[8], electrical impedance spectrometry[9], magnetic relaxation biosensing[10], and a variety of methods based on ellipsometry[11-13]. Currently all of the techniques suffer from at least one of the following drawbacks: lengthy and complex processing for the preparation of linkers to provide robust immobilization of the initial biological recognition layer, non-specific interactions, a short shelf life of pre-prepared sensors, and the lack of a convenient, reliable and rapid diagnosis method[14, 15]. Clearly, an integrated solution is needed that brings together in the sensor design, simple and universal immobilization, storage shelf life and simple diagnosis methodology.

Covalent immobilization of the biomolecular recognition element is preferred, as physically bound biomolecules can be detached during use and often are destabilized by the physical interactions that immobilize them to the surface. Covalent binding is usually achieved with by employing linker groups, which require specialized and complex chemical procedures to prepare them on the surface, and are often not able to retain the activity of the bound molecule over a practically useful time[16-18]. A simple approach that is effective across a broad range of molecules has been recently developed using a thin layer of nitrogen-containing plasma polymer (NPP) to covalently capture protein from solution to immobilize an almost fully dense monolayer of covalent bound, demonstrated using a wide range of proteins and various analysis methodologies[19-24]. Direct evidence for the covalent binding capability of these plasma polymers has been revealed by a shift in the chemical binding energy of the sulfur in cysteine amino groups[22]. The mechanism of the covalent binding of proteins onto the NPP has been attributed to accessible radicals[23, 24]. The covalent binding ability of the NPP was found to last for at least a year

and can be regenerated by annealing in vacuum[19]. The properties of the NPP were characterized previously using the techniques of atomic force microscopy, attenuated total reflection Fourier transform infrared spectrometry, electron paramagnetic resonance, XPS, FTIR, AFM, and surface energy analysis[19-24]. The protein covalent immobilization capability of the NPP plasma polymer was demonstrated using a number of common proteins[19-21], including horseradish peroxidase, human tropoelastin, catalase, and microperoxidase-11.

In this study, we integrate the covalent binding capacity into a complete biosensor methodology in which the recognition proteins are immobilized covalently, followed by freeze-drying to retain their activity during shelf storage. The readout technique we develop in this work is single wavelength, fixed incident angle ellipsometry with optimized sensitivity[13, 25-27]. The advantage of this approach is that the end-users do not need to carry out complex sensor preparation which compromises repeatability and reliability.

Results

Sensing optimization

The concept of our biosensor methodology using ellipsometry is illustrated in figure 1. In Fig.1a, spectra for the ellipsometric parameter Psi are calculated for 3 example sensors with different thicknesses of the NPP layer on a 150 nm silicon nitride coated silicon wafer support. The sensors are assumed to be in a water ambient with sensing radiation inclined at an incidence angle of 70^{o}. The positions of the valleys in the spectra correspond to the wavelengths that give a pseudo-Brewster angle of 70^{o}. The sensitivity, shown by the change in Psi caused by adding a 1.0 nm thick protein layer of refractive index of 1.46, is plotted in Fig 1b. The sensitivity near the valley is low and varies significantly ; therefore, it is necessary to choose the NPP thickness to avoid locating the valley of the Psi spectrum near the 632 nm sensing wavelength. The sensitivity is high and stable for wavelengths that are far well away from the valley. For comparison, the sensitivity (the change of Psi) of a conventional silicon sensor with a self-assembled

monolayer linker layer of 1.0 nm thickness is also shown (Fig 1b). These results show that with an appropriately designed sensor structure, the sensitivity of the sensor can be made much higher than for a silicon sensor with a conventional self-assembled monolayer as a linker. Figure 1c shows the flow chart of the proposed biosensor methodology using the antigen-antibody interaction as an example: design and construct a biosensor according to the principle shown in Fig.1a and Fig.1b with an NPP top layer; covalently immobilize antigen on the biosensor (as in immnosensor); carry out a freeze-drying treatment; store the freeze-dried sensors in dry air; and finally, when needed, use the sensor for diagnosis.

Linker-free covalent immobilization of proteins on plasma polymers

Figure 2 shows some of the examples of linker free protein covalent binding on NPP surfaces and compares them with reference surfaces. Some technical information is provided in SI and illustrated in the Fig.S1-S4. The covalent binding of the proteins to the surfaces was verified by its persistence when exposed to rigorous washing in SDS detergent. In Fig.2a, we show the XPS analysis data of human tropoelastin on NPP compared with bare silicon and diamond-like carbon (DLC). In the XPS analysis, the S 2p peak was used instead of the N 1s peak as the nitrogen peak has a major contribution from the NPP. The XPS S 2p peak arises from cysteine or methionine amino groups in the proteins. Rinsing in water after SDS treatment removes almost all SDS molecules. Any trace or small quantity of remaining unwashed SDS on surfaces can subtracted from the S 2p peak as the binding energy of S 2p in SDS is approximately 4-5 eV larger than that of the main S 2p peak of proteins. This method was recommended previously for XPS analysis of immobilized proteins on surfaces containing nitrogen and the results correlated very well with ELISA analysis[23]. The covalent binding capacity (vertical axis in Fig 2a) is defined as the ratio of the remaining tropoelastin after SDS cleaning to the protein quantity before SDS treatment. A significantly higher covalent binding capacity of the NPP surface was evident. The DLC surface has been previously proposed for biosensor applications, for example, by Hartl *et al*[28]. The significantly higher covalent protein binding capacity of NPP suggests that the NPP surfaces are more suitable for biosensor applications. Fig.2b shows the ellipsometry analysis of catalase on NPP in

buffer with the sequence: without protein (NPP), after incubation in catalase protein solution followed by rinsing with fresh buffer (Cata), after 0.2% SDS treatment without water rinse (SDS), and after rinsing with deionised water (Rinse). Figure 2c shows the quartz crystal microbalance with dissipation (QCMD) analysis of horseradish peroxidase (HRP) on a NPP surface with the sequence: HRP immobilization from solution (HRP), PBS rinse (buffer), 2% SDS cleaning (SDS), then PBS rinse again. The bound mass after SDS treatment and PBS rinse was about 300 ng/cm^2, which is approximately equal to a monolayer of HRP. After introducing SDS, the mass increased initially to approximately twice the mass of the initially immobilized proteins, followed by a steady reduction of the mass. Protein collagen 1 was also analysed using QCMD as shown in Fig.S6 of Supplementary Information (SI), showing a similar result. The ellipsometry result in Fig.2b was also confirmed using XPS analysis, as shown in Fig.S7 of SI.

Figure 2d shows XPS analysis of BMP-7 (human bone morphogenic protein-7) remaining after SDS cleaning using the same analysis method as for Fig.2a. Three surfaces were compared: bare PDMS, plasma polymer without nitrogen (PP), and NPP. The PDMS had negligible covalent binding capacity, the plasma polymer (PP) that contained no nitrogen had a lower covalent binding capacity for the BMP-7 protein than NPP, consistent with previous observations using other proteins[23]. The high coverage of the covalent or strong binding of the proteins on the NPP surfaces provides a straightforward and reliable platform for biosensor applications[29-31].

Table 1 summarizes the proteins used and the method adopted for a range of covalent binding studies together with the covalent binding coverage observed on the NPP surfaces. The high covalent binding capacity for a variety of proteins on the NPP surfaces is attributed to a high density of highly reactive radicals contained within the NPP surfaces[22].

Freeze-drying effect on protein binding

In the freeze-drying treatment, sucrose was used in the last step as a stabilizer. Sucrose and other sugars have been used successfully to stabilize freeze-dried non-immobilized

proteins[32, 33] and linker layers[34] and to retain the activity of freeze-dried HRP immobilized on ion implantation treated polymers[35]. Figure 3a shows the activity as a function of the number of days of rocking in buffer for HRP immobilized on NPP surfaces before freeze-drying (FD-before), after freeze-drying (FD-after) and for HRP immobilized on silicon surfaces (Si) without freeze-drying. Immediately after freeze-drying, the HRP immobilized on NPP had a comparable activity to that before freeze-drying and much higher than its activity on silicon without freeze drying. After 5 and 10 days of rocking in buffer, the activity of the enzymes with and without freeze-drying on NPP was still high compared with silicon. The enhanced activity and the ability to withstand prolonged buffer rocking was attributed to covalent binding in a native conformation, implying that the freeze-drying process did not change significantly the conformation status of the immobilized proteins on NPP. This may be due to multipoint covalent attachment of HRP proteins on the NPP. It has been suggested that multipoint covalent binding can result in a more rigid conformation of immobilized proteins[35, 36].

Figure 3b shows the conformational status of anti-HRP immobilized and freeze dried on NPP surfaces. The plot shows the time required for the anti-HRP to achieve a binding of an approximate monolayer of HRP as a function of HRP concentration. The results show that the anti-HRP remains functional and is capable of binding HRP at very low concentrations of HRP, of less than 1ng/ml. In Fig.3c, we show the activity of the immobilized HRP as a function of storage time after freeze drying. Storage was performed in dry air in a desiccator with ambient temperature in the range between 10 and 20^{o}C (Australia Sydney autumn-winter season, temperature capped at 20^{o}C using cooling-only air-conditioning). The result indicates that using the freeze-drying method, the enzyme immobilized NPP biosensors can be stored at room temperature under dry conditions for a long period of time, convenient for storage and transportation without refrigeration. If refrigerated storage is used, it is expected that an even longer lifetime of immobilized dried proteins is possible[34, 37]. The freeze-drying did not alter the covalent binding nature of the proteins on the NPP surfaces as shown in Fig.3d, in which four proteins were analysed using XPS including HRP, anti-IgG, anti-HRP, and human tropoelastin. The covalent binding capacities assessed after freeze-drying treatment are

similar to those shown in Table 1 without freeze-drying treatment. This is expected as once a protein is covalently bound to a surface, it should be stable under conditions encountered in the freeze-drying treatment unless the surface itself is unstable. In contrast, in the case of silicon surfaces with self-assembled monolayer linkers, the silicon can gradually oxidize and release the bound self-assembled monolayer linker[38, 39].

Nitrogen-containing plasma polymer biosensors without freeze-drying treatment

The performance of the biosensors was first analysed without introducing the freeze-drying treatment. In the following, we demonstrate experimentally the high sensitivity achievable with ellipsometry that was predicted theoretically above. Figure 4 shows a range of protein interactions using both ellipsometry and XPS methods for sensing. Figure 4a and Fig.4b show the measurements obtained over the sequence of operations: before protein immobilization, after incubation in 200 μg/ml anti human IgG buffer solution and subsequent rinsing in buffer (Anti-IgG), followed by blocking in 1 mg/ml BSA and rinsing in buffer (BSA), then after soaking in 200 μg/ml human antibody and rinsing in buffer (IgG). The biosensor in Fig.4a-b was constructed to place the spectral valley in Psi (the wavelength corresponding to the pseudo-Brewster angle of 70^o) close to 632 nm. As shown in the discussion relating to Figure 1a-b, this is a case where the minimum in Psi lies close to the sensing wavelength of 632nm and therefore a measurement of Psi at this wavelength cannot be used for the biosensor readout. Although the changes in the parameter Del near 632nm were large, they were not uniform with wavelength. This means that single wavelength ellipsometry at 632nm cannot be used for reliably quantifying the protein interactions. Note that the BSA blocking after anti-IgG immobilization did not introduce significant additional shifts in either Psi or Del. This is interpreted as the initial anti-IgG immobilization on the NPP surface resulting in a dense covalently bound monolayer, in a good agreement with the results shown in Fig.2 and reported previously[19-24].

Figure 4c shows the Psi spectra for a correctly constructed biosensor for sensing at 632nm. Figure 4c shows measurements obtained over the sequence of operations: before protein immobilization (NPP), after incubation in 50 μg/ml HRP buffer and subsequent

rinsing in buffer (HRP), followed by incubation in 4 μg/ml anti-HRP buffer and rinsing in buffer (HRP+antiHRP), and then further incubation in 100 μg/ml HRP buffer and rinsing in buffer (HRP+antiHRP+HRP). The resulting changes in Psi are: HRP binding (0.43^o), anti-HRP binding (0.80^o), and no change for further HRP exposure. Since the typical angle sensitivity of a low cost ellipsometry system is better than 0.02^o, this result suggests that the NPP sensor provides reliable analysis. Using a simple linear relationship between the immobilized protein layer thickness and the change of Psi, we can calculate that the molecular ratio of the anti-HRP to initially bound HRP is 1:1.5. This indicates that the anti-HRP captured by the initial immobilized HRP also had a high density. Further incubation in HRP (to give the layer structure HRP+antiHRP+HRP) did not alter the reading. The XPS analysis on the anti-HRP biosensor agreed reasonably well with the ellipsometry data in Fig.4c which gave a value of 1.86 for the immobilized protein quantity ratio of the anti-HRP to the HRP as shown in Fig.4d. The shoulder in the C1s spectra near 288.5eV are commonly used for approximate quantification of immobilized proteins[40]. The integrated intensity ratio in the range of the shoulder for the increment due to additional anti-HRP immobilization to that due to the HRP immobilization was 2.0, which was the approximately the same ratio as that obtained using the corresponding S 2p peaks in the XPS analysis. Considering the fact that in the XPS analysis, a thicker protein surface layer would be slightly over-counted due to the higher sensitivity for the top layer[41] unless only one monolayer layer of proteins is immobilized[23], this is considered good agreement.

In Fig.4e, we show another NPP biosensor using human tropoelastin and anti-tropoelastin and the ellipsometry method for sensor readout (the corresponding spectra were shown in Fig.S9 of SI). The Psi readings at 632 nm shown in Fig.4e are for the following sequence of conditions: before protein immobilization (NPP), after incubation in 20 μg/ml anti human tropoelastin and rinsing in buffer (Anti-tropo), followed by incubation in 5 μg/ml human tropoelastin and rinsing in buffer (Tropo). The corresponding ellipsometry spectra for Fig.4e are shown in Fig.S9 of the SI. The sensitivity for both the anti-tropoelastin and tropoelastin was good, and was smaller than the measurement uncertainty.

In Fig.4f we show the XPS C1s spectra of a NPP biosensor for the following sequence of conditions: before protein immobilization (NPP), after incubation in 20 μg/ml protein-A and rinsing in buffer (PA), and then incubation in 50 μg/ml human IgG and rinsing in buffer (PA+IgG). Protein-A is widely used in biosensors to orient antibodies[42]. The same type of NPP biosensor was also analysed using the ellipsometry method for the same sample sensing conditions. The values of Psi at 632 nm are given in the inset to Fig.4f. Protein-A can accommodate the Fc site of an IgG molecule to leave the Fab sites available for antigen binding reactions. The changes in Psi resulting from the protein immobilization are 0.21^{o} and 0.35^{o} for protein-A and human IgG respectively. Using XPS C 1s analysis, the mass ratio of the immobilized IgG to the protein-A was found to be about 1.64, which agrees well with the ratio 1.66 determined using the ellipsometry method. The XPS and ellipsometry analysis shown in Fig.4f suggests that approximately every two immobilized protein-A proteins can capture one IgG protein, giving approximately a 50% capture efficiency. Considering the larger size of an IgG compared to protein-A, this IgG capture efficiency of the immobilized protein-A is excellent, and it is consistent with the random model of protein adsorption and shows that almost all IgG molecules are correctly oriented.

Freeze-dried nitrogen-containing plasma polymer biosensors

The sensitivity of the freeze-dried NPP biosensors using ellipsometric readout at 632nm is shown in Figure 5. All the freeze-dried NPP biosensors had storage conditions similar to that for Fig.3c with a storage period between one week and two months. The corresponding spectra of Fig.5a-e are shown in Fig.S10 of SI. Figure 5a shows a NPP biosensor for human IgG measured over the sequence of operations: incubation in 20 μg/ml anti-IgG followed by freeze-drying (Anti-IgG+FD), incubation in 1mg/ml BSA blocking (BSA), and the incubation in 10 μg/ml human IgG. After BSA blocking, the reaction with human IgG resulted in a change of Psi approximately 25 times larger than the change from the BSA blocking, demonstrating a high sensitivity of the NPP IgG biosensor.

In Fig.5b we show the operation of a freeze dried protein A biosensor. The sequence of conditions was: protein-A immobilized and freeze dried (PA+FD), 40 μg/ml anti-tropoelastin immobilization (Anti-tropo), 1 mg/ml BSA blocking (BSA), and 40 μg/ml human tropoelastin immobilization (Tropo). As shown in the Figure, the freeze dried biosensor can be functionalised with Anti-tropoelastin and is capable of detecting Tropelastin in solution. Figure 5c shows results for a similar freeze-dried protein-A immobilized NPP biosensor for the human IgG and anti-IgG reaction. The following sequence of operations was used：protein-A immobilization and freeze-drying (PA+FD), 20 μg/ml human IgG immobilization (IgG), 1mg/ml BSA blocking (BSA), 1 μg/ml anti-IgG immobilization (Anti-IgG), and further 20 μg/ml human IgG immobilization (IgG+). The first IgG immobilization resulted a large increment of Psi, indicating the excellent efficiency of the capturing ability of the immobilized and freeze-dried protein-A on the NPP biosensor. The large anti-IgG immobilization increment shows that the function of the IgG is preserved during the immobilization. The stability of the triple-layer of proteins (Protein A+IgG + antiIgG) was challenged by a further soaking in 20 μg/ml human IgG buffer (IgG+) fro 30 min. There was only a small decrease of Psi indicating that the triple-layer was stable.

The effectiveness of the freeze-drying was further analysed using a NPP biosensor which was processed with protein-A immobilization and then human IgG soaking prior to the freeze-drying treatment. In Fig.5d, we show the response of the biosensor in the analysis with the sequence of operations：after protein-A and human IgG immobilization then freeze-drying treatment (PA+IgG+FD), 1 mg/ml BSA blocking (BSA), then 10 μg/ml antiIgG immobilization (Anti-IgG). The biological responses of this biosensor were similar to those in Fig.5a-c. Such freeze-dried protein double-layer biosensors provide an opportunity for a wide range of end-users and applications and will have a particular advantage when rare antigen (or antibody) biosensors are required in medical diagnosis. In Fig.5e we show a HRP immobilized biosensor with the sequence of operations：after HRP immobilization and freeze-drying treatment (HRP+FD), 1 mg/ml BSA blocking

(BSA), then 4 μg/ml anti-HRP immobilization (Anti-HRP). The biological responses of the anti-HRP biosensor were consistent with the performance of other biosensors described above (Fig.5a-d). Figure 5f is an example of a time trace of Psi for an anti-HRP biosensor, showing the response of the anti-HRP immobilization. After approximately 30 minutes, the antigen-antibody reaction was sufficient for the Psi signal to stabilize in a conveniently short time even when a low (0.2 μg/ml) concentration of anti-HRP was used.

Discussion and conclusions

We have demonstrated in this paper an integrated solution for biosensing. The methodology we have demonstrated is reliable, rapid, and the end-user will find it easy to use. The reliability of the biosensors results from the high covalent binding capacity of the NPP surfaces for protein and the excellent performance of the biosensors after a freeze-drying treatment. The rapidity and the end-user convenience are attributed to the optimized biosensor optical design, the simplicity of the diagnosis method, and the simple storage procedure, enabling minimal involvement at the diagnosis step, especially for those not having specific biosensor formation facilities and skills. XPS and QCMD were used to confirm the covalent binding nature of the NPP surface before and after the freeze-drying treatment. The antigen-antibody interactions on the NPP biosensors were comprehensively reconfirmed after freeze drying using the XPS technique.

Three different pairs of antigen-antibodies, together with protein-A to accommodate different antibodies, were tested to demonstrate the new biosensor methodology. It is apparent that this method is suited for not only immunosensors but also for other types of biosensors as long as the biological reactions result in mass change or involve molecular binding/detaching processes on the surface of the biosensor. The high sensitivity of the biosensors using the antigen-antibody interactions was demonstrated consistently for cases with and without freeze-drying treatment. Protien-A after covalent immobilization remained functional for the cases: protein-A only with and without freeze-drying treatment, and antibody on protein-A with freeze-drying treatment. BSA blocking showed very little changes of sensor readings, compared to those resulting from the

antigen-antibody interactions, indicating a high density of covalently immobilized functional protein for all cases with or without freeze-drying treatment. Using anti-HRP biosensors for consistency analysis, we found the ratio of sensing signal to BSA blocking signal was basically higher than ten, and the signal induced by BSA blocking was almost all within system errors (showing in Figure S11 of SI).

The ellipsometry Psi signal ratios of antibody to antigen in the biosensor diagnosis were consistent with dense layers of antibody or antigen captured or immobilized, as shown in Fig.4a, 4c, 4e-f, and Fig.5b-c. The uniform response in a wide range of wavelengths, in the vicinity of aimed single wavelength 632 nm proves that the biosensor sensitivity can be controlled with minimal influence from variations in NPP thickness, providing a convenience approach for formation of standardized biosensors.

The typical data collection time for ellipsometry analysis (single wavelength and single biological reaction step) for each biosensor is expected to be within a few minutes in most cases. Most of the processing time in the biosensor diagnosis in the ellipsometry method is the time required for the biological reaction to stabilise or complete, which is approximately one hour. This means in the biosensor applications the bottle-neck to limit the biosensor diagnosis throughput is not the data collection. Using the standardization of the NPP biosensors, a fast throughput of biosensor diagnosis can be achieved by rapidly rotating biosensors through a simple ellipsometry analysis unit while waiting for the biological reactions to complete. This can offer a convenient and low cost solution for matching the speed advantage of integrated diagnosis techniques such as imaging ellipsometry[43, 44], which however is disadvantaged with its high cost and complication in data analysis. In addition, as the NPP biosensor process and properties were found to be compatible with the standard CMOS semiconductor integrated device technology[19], the NPP biosensor methodology thus can be also used for integrated and miniature biosensors whenever this becomes necessary.

The reasons for the high covalent protein binding capacity of the NPP surfaces compared with the DLC surfaces were investigated. The covalent protein binding effect of plasma

polymers or plasma modified polymers was recently proposed and demonstrated experimentally to result from not only the areal density of radicals in the surfaces but also the mobility of the radicals[24]. The radical density of the DLC surfaces was found using EPR to be similar to that of the NPP surfaces. Thus the lower covalent protein binding capacity of the DLC surfaces could result from its significantly lower radical mobility as suggested in the EPR analysis, which is consistent with the one-dimensional quantum well model in our theoretical simulation for the radical transportation and protein covalent binding enhancement (Fig.S12 of SI)

In summary, an integrated solution for a versatile biosensor technology has been demonstrated with the desirable features of long shelf life, simple storage procedure, reliable performance and minimal involvement of end-users. The technology combines the high protein covalent binding capacity of NPP surfaces with a high sensitivity, low cost diagnosis method that shows robust performance after freeze-drying. The covalent binding mechanism of the NPP surface was investigated by EPR spectroscopy. A model in which mobile electron spins are responsible for both the EPR signal and the covalent binding was confirmed. The merits of the technology were demonstrated experimentally using three antigen-antibody pairs.

ACKNOWLEDGEMENTS

We acknowledge financial support from Australian Research Council. We gratefully acknowledge technical discussion with Professors C.G. dos Remedios, J. Gooding, H.G.L. Coster and H. Yasuda, Drs W.R. Yang, D. Reilly, D. Bax and T. Chilcott.

COMPETING FINACIAL INTERESTS

The authors declare no competing financial interests.

References

1. Stayton, P.S. et al, Control of protein–ligand recognition using a stimuli-responsive polymer, Nature, 378, 472-474 (1995).
2. Victor, S.Y. et al. A porous silicon-based opticalinterferometric biosensor, Science, 278, 840-843 (1997).
3. Schena, M. et al. Quantitative monitoring of gene expression patterns with a complementary DNA microarray, Science, 270, 467-470 (1995).
4. Southern, E.M. et al. Arrays of complementary oligonucleotides for analysing hybridization behaviour of nucleic acids, Nucleic Acids Res. 22, 1368-1373 (1994).
5. Lee, J.W. et al. Interaction of thyroid-hormone receptor with a conserved transcriptional mediator, Nature, 374, 91-94 (1995).
6. Kuno, A. et al. Evanescent-field fluorescence-assisted lectin microarray: a new strategy for glycan profiling, Nature Methods, 2, 851-856 (2005).
7. Bornhop, D.J. et al. Free-solution, label-free molecular interactions studied by back-scattering interferometry, Science, 317, 1732-1736 (2007).
8. Shekhawat, G. et al. MOSFET-embedded microcantilevers for measuring deflection in biomolecular sensors, Science, 311, 1592-1595 (2006).
9. Giaever, I. and Keese, C. R. A morphological biosensor for mammalian cells, Nature, 366, 591-592 (1993).
10. Perez, J.M. et al. Magnetic relaxation switches capable of sensing molecular interactions, Nature Biotechnology, 20, 816-820 (2002).
11. Schuster, S.C. et al, Assembly and function of a quaternary signal transduction complex monitored by surface plasma resonance, Nature, 365, 343-347 91993).
12. Jin, G. et al. A biosensor concept based on imaging ellipsometry for visualization of biomolecular interactions, Anal. Biochem. 232, 69-72 91995).
13. Striebel, Ch. Et al, Characterization of biomembrranes by spectral ellipsometry, surface plasma resonance and interferometry with regard to biosensor application, Biosensors & Bioelectronics, 9, 139-146 (1994).

14. Wu, G et al. Bioassay of prostate-specific antigen (PSA) using microcantilevers, Nature Biotechnology, 19, 856-860 (2001).
15. Mok, W and Li, Y. Recent progress in nucleic acid aptamer-based biosensors and bioassays, Sensors, 8, 7050-7084 (2008).
16. Radadia, A.D. et al. Biosensors: Control of nanoscale environment to improve stability of immobilized proteins on diamond surfaces, Adv. Funct. Mater. 21, 1008-1010 (2008).
17. Fletcher, S.J. et al. Toward specific detection of Dengue virus serotypes using a novel modular biosensor, Biosensors & Bioelectronics, 26, 1696-1700 (2010).
18. Zheng, L. et al. Bilayer lipid membrane biosensor with enhanced stability for amperometric determination of hydrogen peroxide, Talanta, 85, 43-48 (2011).
19. Yin, Y. et al. Plasma polymer surfaces compatible with CMOS process for directly covalent enzyme immobilization, Plasma Processes & Polymer, 6, 68-75 (2009).
20. Yin, Y. et al. Covalent immobilisation of tropoelastin on a plasma deposited interface for enhancement of endothelialisation on metal surfaces, *Biomaterials*, 30, 1675–1681 (2009).
21. Yin, Y. et al. Direct evidence of covalent immobilisation of microperoxidase-11 on plasma polymer surfaces, *Plasma Processes and Polymers*, 7, 708–714 (2010).
22. Yin, Y. et al. Covalently bound biomimetic layers on plasma polymers with graded metallic interfaces for in vivo implants, *Plasma Process. Polym.* 6, 658-666 (2009).
23. Yin, Y. et al. Protein immobilization capacity and covalent binding coverage of pulsed plasma polymer surfaces, *Applied Surface Science*, 256, 4984-4989 (2010).
24. Bilek, M.M.M. et al, Free radical fictionalization of surfaces to prevent adverse response to biomedical devices, PNAS, doi/10.1073/pnas.1103277108.
25. Arwin, H. Is ellipsometry suitable for sensor applications? Sensors and Actuators, 92, 43-51 (2001).
26. Nirschl, M. et al. CMOS-integrated film bulk acoustic resonators for label-free biosensing, *Sensors*, 10, 4180-4193 (2010).

27. Yin, Y. et al. Elipsometry analysis of conformational change of immobilized protein monolayer on plasma polymer surfaces, *Thin Solid Films*, 519, 2968-2971 (2011).
28. Hartl, A. et al. Protein-modified nanocrystalline diamond thin films for biosensor applications, Nature Materials, 3, 736-742 (2004).
29. Wink, T. et al. Self-assembled monolayers for biosensors, *Analyst,* 122, R43-50 (1997).
30. Williams, R.A. and Blanch, H.W. Covalent immobilization of protein monolayers for biosensor applications, *Biosensors & Bioelectronics*, 9, 159-167 (1994).
31. Bilek, M.M.M. and McKenzie, D.R. Plasma modified surfaces for covalent immobilization of functional biomolecules in the absence of chemical linkers: towards better biosensors and a new generation of medical implants, Biophy. Rev., 2, 55-65 (2010).
32. Carpenter, J.F. et al. Stabilization of phosphofructokinase with sugars during freeze-drying: characterization of enhanced protection in the presence of divalent cations, Biochimica et Biophysica Acta-General Subjects, 923, 109-115 (1987).
33. Buchinger, S. et al. Development of freeze-drying protocol for the long-term storage of S9-fraction at ambient temperature, Cryobiology, 58, 139-144 (2009).
34. Xia, N. et al. A streptavidin linker layer that functions after drying, Langmuir, 20, 3710-3716 (2004).
35. Bes, T. et al. Selective enzymetic oxidations: stabilization by multipoint covalent attachment of ferredoxin NAD-reductasa: an interesting cofactor recycling enzyme, J. Mol. Catal. 98, 161-169 (1995).
36. Fernandez-Lafuente, R. et al. Hyperstablization of a thermophilic esterase by multipoint covalent attachment, Enzyme Microb. Technol. 17, 366-372 (1995).
37. Nosworthy, N.J. et al. A new surface for immobilizing and maintaining the function of enzymes in a freeze-dried state, 10, 2577-2583 (2009).
38. Schlenoff, J.B. et al. Stability and self-exchanged in alkanethiol monolayers, J. Am. Chem. Sco. 117, 12528-12536 (1995).

39. Mrksich, M. et al. Using microcontact printing to pattern the attachment of mammalian cells to self-assembled monolayers of alkanethiolates on transparent films of gold and silver, Exp. Cell Res. 235, 305-313 (1997).
40. Wagmer, M. S. et al. Limites of detection for time of flight secondary ion mass spectrometry (TOF-SIMS) and X-ray photoelectron spectroscopy (XPS): detection of low amount of adsorbed proteins, J. Biomater. Sci. Polymer Edn, 13, 407-428 (2002).
41. Lubambo, A.F. et al. Adsorption of protein GInB of herbaspirillum seropediceae on Si (111) investigated by AFM and XPS, Cell Biochem. Biophys. 44, 503-511 (2006).
42. Muramatsu, H. et al. Piezoeletric crystal biosensor modified with protein A for determination of immunoglobulins, Anal. Chem. 59, 2760-2763 (1987).
43. Qi, C. et al. Detection of avian influenza virus subtype H5 using a biosensor based on imaging ellipsometry, Biosensors & Bioelectronics, 25, 1530-1534 (2010)
44. Jin, G. et al. Imaging ellipsometry revisited: Developments for visualization of thin transparent layers on silicon substrates, Rev. Sci. Instrum. 67, 2930-2936 (1996).

Methods

Plasma polymer deposition

The plasma polymer method and system was reported previously[19, 45]. The schematic diagram of the system is given in the supplementary materials (Fig.S1). Briefly, the NPP deposition system included two plasma sources: one radio frequency (RF) electrode at 13.56 MHz operated at 120 W to generate background plasma; the other one was a substrate holder connected to a pulse voltage source at 200V with pulse length 10 μs and repetition 10 kHz. Gases injected into the plasma chamber were acetylene (10 sccm), nitrogen (4 sccm), and argon (4 sccm). Pressure of the system was maintained at 20 Pa. During NPP deposition, the substrate temperature was uncontrolled and lower than approximately 60^{o}C.

Freeze-drying method for end-user ready biosensors

The freezing-drying method adopted in this work was similar to that reported by Nosworthy *et al*[37], 2.5% sucrose in buffer was added prior to freezing to stabilize the immobilized proteins. The procedure in this work was: first the protein immobilized plasma polymer surfaces were rinsed and transferred to Falcon tubes containing 2.5% sucrose in PBS buffer, each tube contained one NPP biosensor with 2 ml the sucrose containing buffer, then the tubes were placed into liquid nitrogen and the samples were frozen. Once frozen, the samples were transferred to a drying chamber (a Christ Alpha 2-4 LDplus freeze dryer) with 0.3 mbar pressure for 48 hours until the drying process was completed. The samples were then stored in a desiccant with Sigma silica drying agent. The desiccated samples were stored at room temperature capped at 20^{o}C with a non-heating air conditioning during the autumn-winter seasons at Sydney, Australia (5-25^{o}C).

Materials and bio-assays

Proteins tested and chemicals used were all purchased from Sigma without further purification except human tropoelastin, including horseradish peroxidase (Cat No P6782), bovine liver catalase (Cat No C3155), calf skin collagen 1 (Cat No C9791), Microperoxidase-11 (Cat No M6756), BMP 7 (Cat No B1434), human serum IgG (Cat

No I4506), anti-human IgG (Cat No I3266), protein-A (Cat No P1406), HRP antibody (Cat No P7899). Human (recombinant) tropoelastin corresponding to amino acid residues 27–724 of GenBank entry AAC98394 (gi 182020) was expressed and purified as previously described[46], tetramethylbenzidine (TMB, 3,3′,5,5′ tetramethylbenzidine, Cat No T0440), and anti-elastin (called anti-tropoelastin in the text)) clone BA-4 antibody (Cat No E4013).

The procedure for HRP attachment and activity analysis is as follows unless specified in the text. Samples were incubated for 20 hours in HRP (50 µg/ml) in 10 mM phosphate buffer (PB) at pH 7.0. Incubations were in 75 mm sterile Petri dishes with rocking. After the incubation, the samples were washed 6 times each for 20 minutes in 10 mM phosphate buffer pH 7.0. The first wash was performed in the Petri dish used for enzyme incubations. Then the samples were transferred to a clean Petri dish for the next 5 washes. Active HRP on the surfaces of the samples was measured by clamping the sample (approx 15x15 mm) between two stainless plates separated by an O-ring (inner diameter 8.0 mm, outer diameter 11.0 mm) that sealed the surface. The top plate contained a 5.0 mm diameter hole enabling the addition of 75 µl of the HRP enzyme substrate, TMB. After 30 seconds (or the duration specified in the text), 25 µl of reacted TMB was taken and added to 50 µl of 2 M hydrochloric acid to stop the reaction. A further 25 µl of unreacted TMB was then added to bring the volume to 100 µl. The absorbance of the solution at 450 nm was then measured using a Beckman DU530 Life Science UV/VIS spectrophotometer. All enzyme activity tests including rocking time were performed at 23 ± 1^{o}C. SDS cleaning in XPS analysis to remove physically immobilised proteins was carried out using 2% SDS in Milli-Q water and rocking for 4 hours at 70^{o}C followed by rinsing in water for 5 times each 5 minutes. SDS cleaning in ellipsometry analysis was conducted at room temperature with the procedure specified in the text and supplementary materials.

Biosensor diagnosis methods

The NPP biosensors were characterized using J.A. Woollam M-2000 spectroscopic ellipsometry, which allows us to obtain complete information in a wide range of

wavelengths, including wavelength at 632 nm. The ellipsometry system is with typical sensitivity and accuracy ($\pm 0.01^{o}$ for Psi) and has been demonstrated its effectiveness in many analysis[27, 47, 48]. A flow cell with 70^{o} incidence angle windows was used during the ellipsometry analysis. All ellipsometry analysis was done at 70^{o} incident angle. Soaking for protein immobilization or interaction was all conducted for 30 minutes unless specified in the text. A photoelectron spectroscopy (XPS) system, (model: SPECS-XPS, from SPECS, Germany) was used to analyze the element concentration and binding energies of the plasma polymer surfaces. The XPS system was equipped with a high sensitivity PHOIBOS 150-9 MCD energy analyzer, capable of detecting medium sensitivity elements to a trace level in an order of 100ppm. Al K-alpha X-ray source (1486.74eV) was used in the analysis.

References for methods

45. Yin, Y. *et al*. Acetylene Plasma Polymerised Surfaces for Covalent Immobilization of Dense Bioactive Protein Monolayers, Surf. Coatings & Techno., 203, 1310-1316 (2009).
46. Wu, W.J. *et al*. Glycosaminoglycans mediate the coacervation of human tropoelastin through dominant charge interactions involving lysine side chains, J Biol. Chem. 274, 21719–21724 (1999).
47. Fujiwara, H. *et al*. Real-time spectroscopic ellipsometry studies of the nucleation and grain growth processes in microcrystalline silicon thin films, Phys. Rev. B, 63, 115306-115314 (2001).
48. Arwin, A. *et al*. Infrared Ellipsometry Studies of Thermal Stability of Protein Monolayers and Multilayers, *Phys. Stat. Sol.* 5, 1438-1441 (2008).

Figure captions

Figure 1: (a) the ellipsometry spectra of Psi for sensors with different NPP layer thickness, (b) the sensitivity, or the change of Psi by 1 nm thick proteins, for the sensors in (a) as a function of wavelength, together for a silicon sensor with an 1nm thick self-assembled monolayer linker, (c) the flow chart of the sensing methodology using antigen-antibody as the example: design and formation of a base sensor with activated polymer surface; attach antigen; freeze-dry; store in dry air; then use by end-user for diagnosis.

Figure 2: Analysis of covalent binding of proteins determined using SDS detergent washing, (a) XPS analysis of human tropoelastin on bare silicon, diamond-like carbon (DLC), and nitrogen-containing plasma polymer (NPP); (b) ellipsometry analysis of catalase on NPP in buffer with a sequence of without protein (NPP), after protein and then rinse (Cata), 0.2% SDS without rinse (SDS), after rinse (Rinse), (c) QCMD analysis of HRP on NPP surface, (d) XPS analysis of remaining BMP-7 after SDS cleaning on bare PDMS, plasma polymer without nitrogen (PP), and NPP, quantified using S 2p peaks.

Figure 3: The effect of freeze-dry on the conformation of the immobilized proteins and protein binding strength, (a) the activity of immobilized HRP as a function of time in PB buffer for surfaces of silicon without freeze-drying (Si), NPP without freeze-drying (FD-before), and NPP with freeze-dry after HRP immobilization (FD-after); (b) the time required for activity to reach 0.5 for immobilized HRP onto anti-HRP attached and freeze-dried NPP surfaces as a function of HRP concentration, showing the freeze-dried and immobilized anti-HRP biosensors were highly sensitive to a small trace of HRP in buffer; (c) the retained activity of immobilized HRP on NPP for conditions of without freeze-dry (No FD), immediately after freeze-dry (FD 0 day), and three months after freeze-dry (FD 3 months); (d) covalent binding

capacity for four examples of proteins immobilized onto NPP surfaces after freeze-dry process and analyzed using XPS.

Figure 4: Applications of the proposed biosensors for different antigen-antibody interactions using the ellipsometry and XPS diagnosis methods, (a) and (b) elipsometry spectra of Psi and Del respectively in the range near 632nm for sequential conditions: before protein immobilization on NPP (NPP), after anti human IgG soaking in 200 μg/ml buffer and rinse (Anti-IgG), followed by soaking in 1mg/ml BSA solution (BSA), then soaking in 200 μg/ml human antibody (IgG); (c) ellipsometry Psi spectra and (d) XPS C 1s spectra for biosensors before protein immobilization (NPP), soaking in 50 μg/ml HRP buffer (HRP), after 4 μg/ml anti-HRP buffer (HRP+antiHRP); then further soaking in 100 μg/ml HRP buffer and rinse (HRP+antiHRP+HRP); (e) the Psi readings at 632 nm for a biosensor at conditions: no protein immobilization (NPP), after 20 μg/ml anti human tropoelastin immobilization and rinse (Anti-tropo), and then after 50μg/ml human tropoelastin immobilization and rinse (Tropo); (f) XPS C 1s spectra of biosensors for conditions: before protein immobilization (NPP), after 20μg/ml protein-A immobilization and rinse (PA), and then further 50 μg/ml human IgG soaking and rinse (PA+IgG), the values of Psi in the legends' brackets are the ellipsometry analysis data for the same conditions at 632 nm wavelength.

Figure 5: Examples of biosensors with freeze-drying treatment using ellipsometry analysis (note all steps from (a) to (e) had buffer rinse). (a) a human IgG biosensor on anti-IgG immobilized biosensor with a sequence of after anti-IgG immobilization and freeze-dry (Anti-IgG+FD), BSA blocking (BSA), and human IgG immobilization; (b) a protein-A immobilized biosensor with a sequence of after protein-A immobilization and freeze-dry treatment (PA+FD), anti-tropoelastin immobilization (Anti-tropo), BSA blocking (BSA), and human tropoelastin immobilization (Tropo); (c) a

protein-A immobilized biosensor with a sequence of after protein-A immobilization and freeze-dry treatment (PA+FD), human IgG immobilization (IgG), BSA blocking (BSA), anti-IgG immobilization (Anti-IgG), and further human IgG immobilization (IgG+); (d) a protein-A then human IgG immobilized biosensor with a sequence of after protein-A and human IgG immobilization then freeze-dry treatment (PA+IgG+FD), BSA blocking (BSA), then antiIgG immobilization (Anti-IgG); (e) a HRP immobilized biosensor with a sequence of after HRP immobilization and freeze-dry treatment (HRP+FD), BSA blocking (BSA), then anti-HRP immobilization (Anti-HRP); (f) a time trace of Psi at 632 nm for an anti-HRP biosensor, showing the response of the anti-HRP immobilization.

Figures and Tables

Figure 1

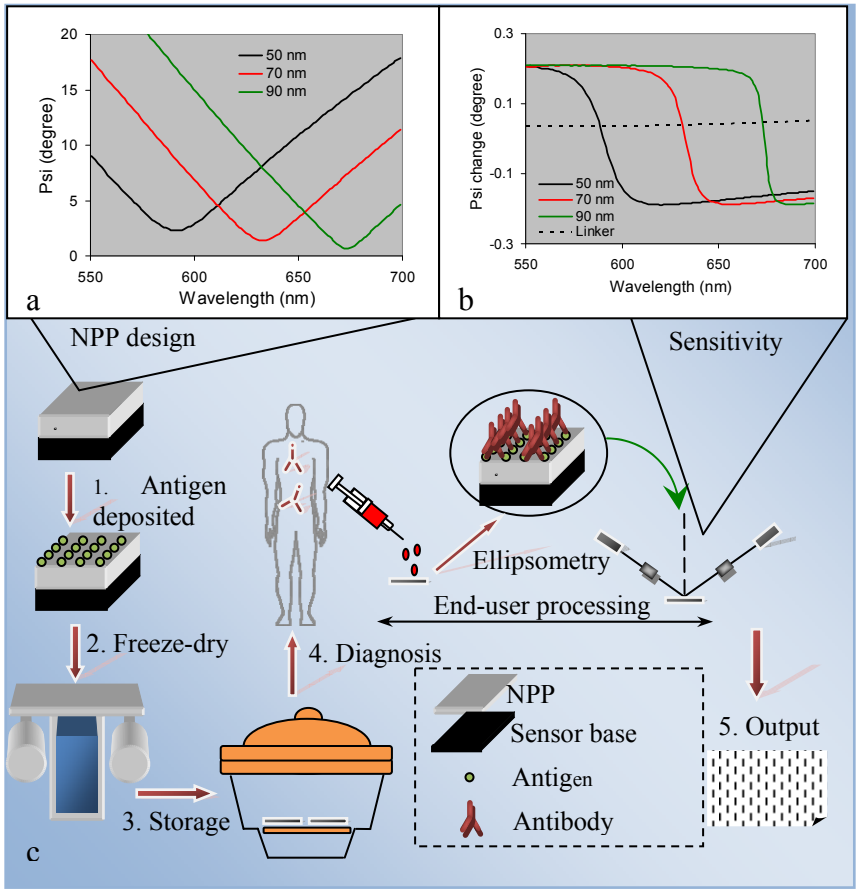

Figure 2

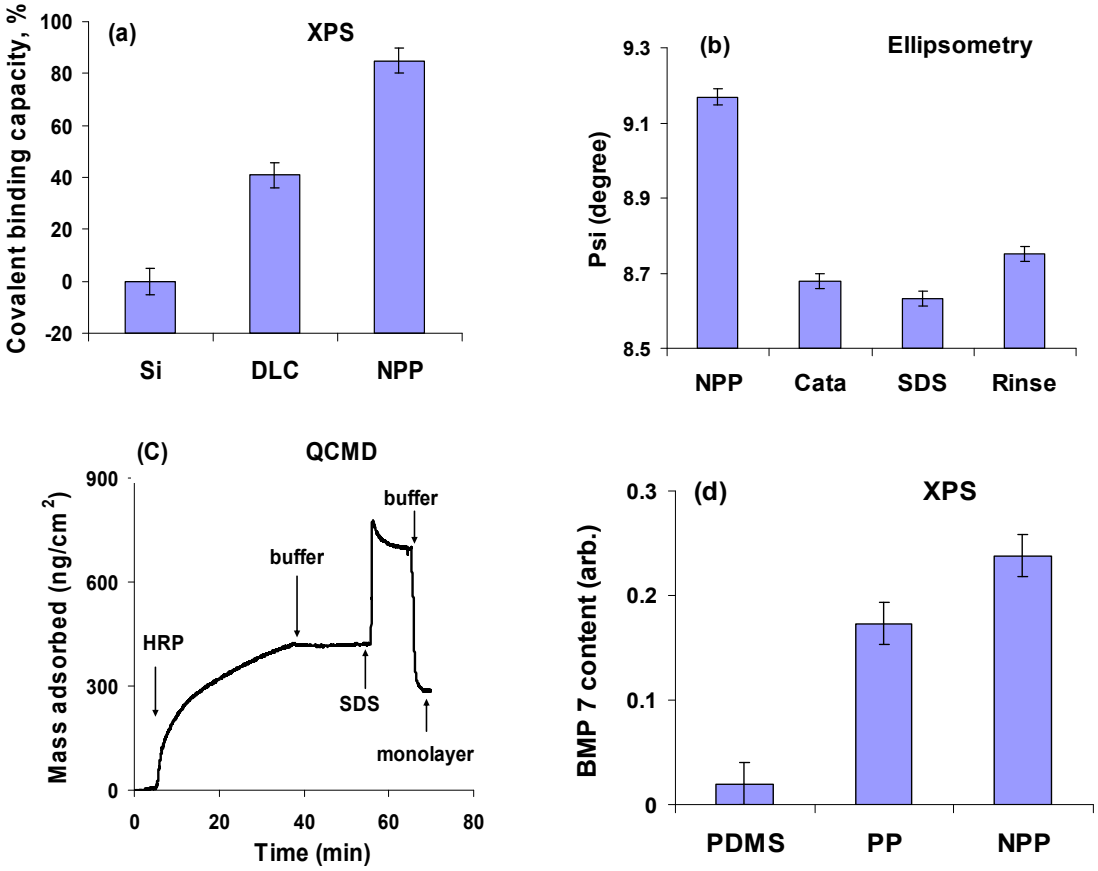

Figure 3

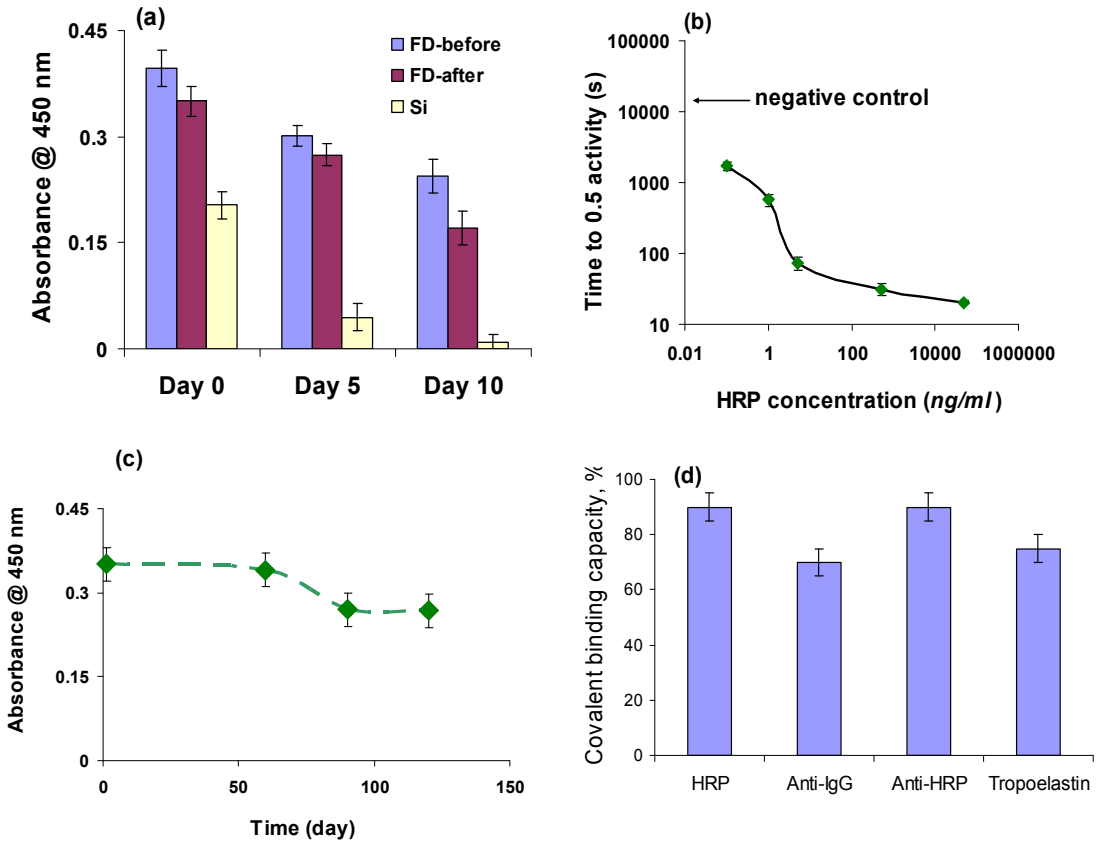

Figure 4

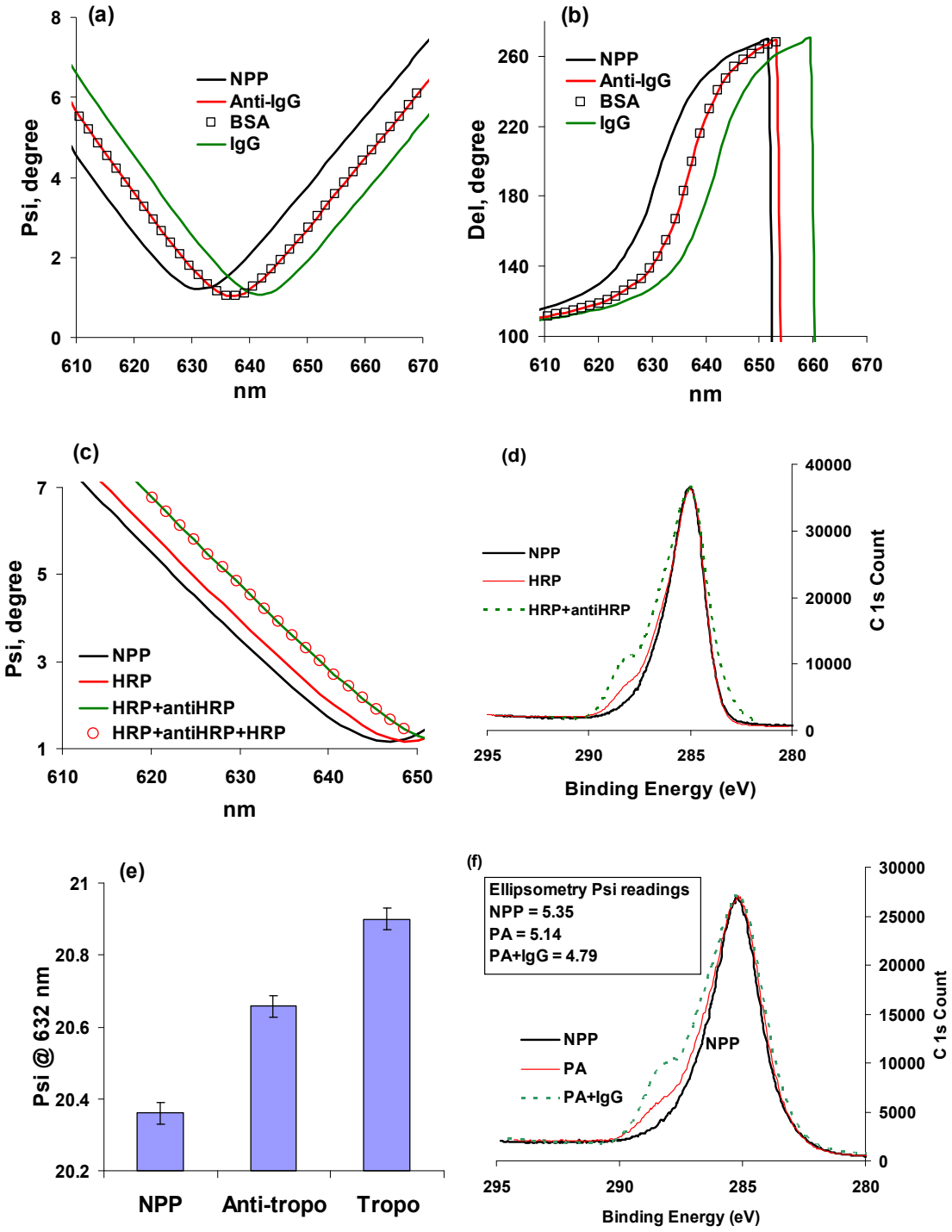

Figure 5

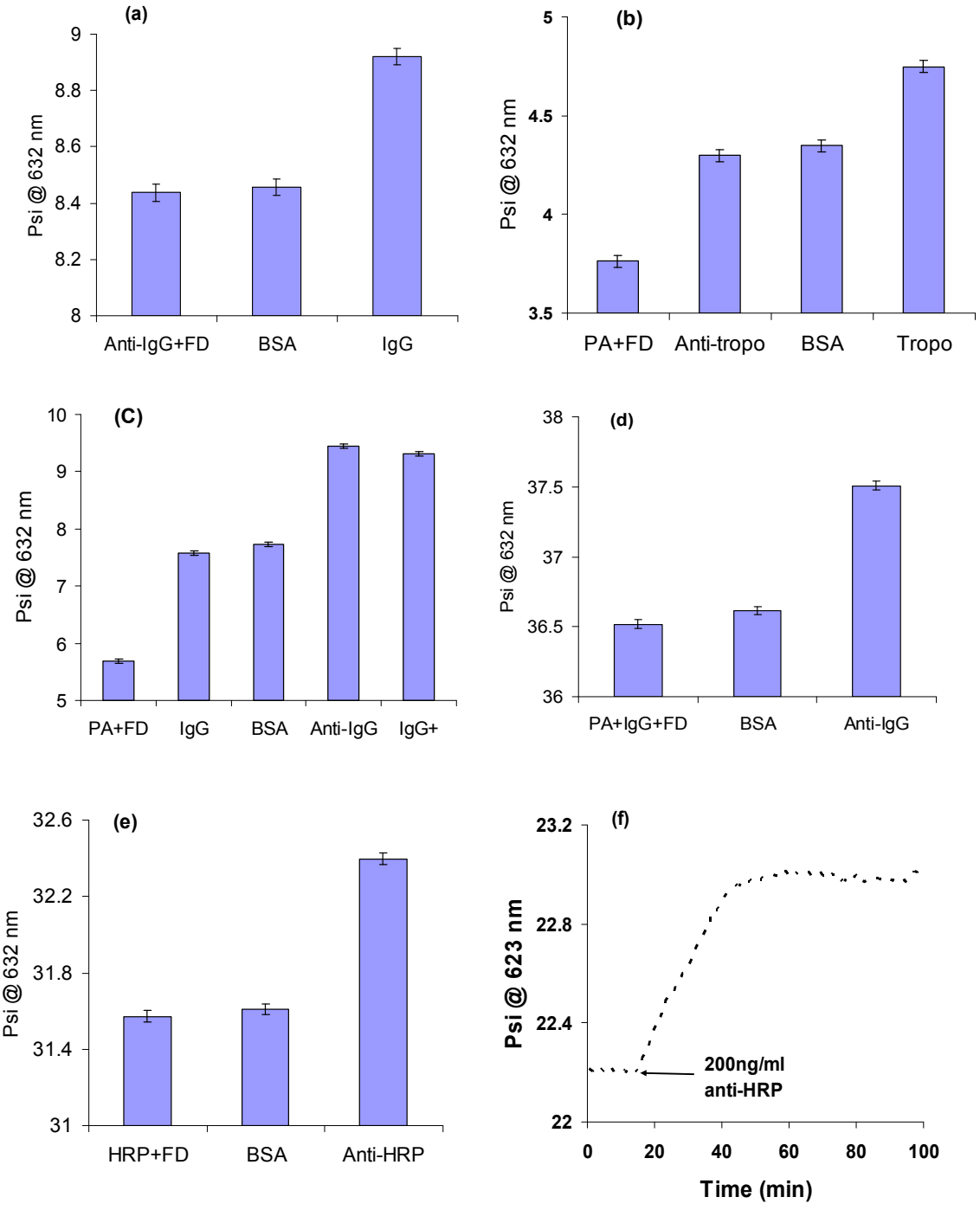

Table 1: Covalent binding coverage of a variety of proteins on the NPP surfaces using different analysis methods, the sign of * indicates the test was reported previously in references 19-23.

Protein	Methodology	Covalent coverage
human tropoelastin	XPS*, QCMD*, ELISA*	≥75%
bovine liver catalase	XPS*, QCMD*, Ellipsometry	≥75%
horseradish peroxidase	XPS*, QCMD*, Ellipsometry	≥75%
microperoxidase-11	XPS*	≥80%
bone morphogenic protein-7	XPS	≥75%
calf collagen 1	Ellipsometry, QCMD, XPS	≥80%
Anti human IgG	XPS, Ellipsometry	≥75%